

## Supplementary materials

### Materials and Methods

#### Materials

AAM, MEDSAH and hydroquinone were purchased from Sigma-Aldrich (St. Louis, MO). *N,N'* methylene bis(acrylamide), triethanolamine (TEOHA), and riboflavin were obtained from Neta Scientific (Hainesport, NJ). Iron oxide (Fe<sub>3</sub>O<sub>4</sub> high purity) nanoparticles (15-20 nm, 20 wt % suspension in water) were supplied by US Research Nanomaterials, Inc. (Houston, TX). All reagents were used as received without further purification.

The zwitterionic formulations typically consist of AAM and MEDSAH in the weight ratio of 50:50. Certain amounts of MBA, according to DOE, were added into the pre-gel solutions. The solutions were then sonicated in a water bath until all components are dissolved. Solutions were kept in the dark until riboflavin and TEHOA were added immediately before use. During the 3D printing, hydroquinone was added, at 180 μL (1 mg mL<sup>-1</sup>) per 50 mL pre-gel solution, as a radical scavenger to terminate active species and restrict the polymerization to illuminated regions. Additionally, iron (II, III) oxide nanoparticles were added as light absorbing material at low concentrations (~0.05 to 0.07 wt%). The role of iron oxide NPs is to act as light absorbing agents and prevent light from penetrating too deep into previously formed layers, which improves printing resolution.

## **Stereolithography**

We used the Ember (Autodesk Inc., San Rafael, CA) digital mask projection SLA 3D printer, equipped with a 405 nm light emitting diode (LED) projector as the light source, for the fabrication of the zwitterionic demo hydrogel [1]. A transparent polymethylpentene window was installed at the bottom of the resin tray for SLA. The photoirradiation density is around 22.5 mW cm<sup>-2</sup>. The octopus CAD file was obtained freely under a creative commons license.

The 3D printing process and the related parameters were controlled by the Autodesk Print Studio software, with a thickness from 50 to 100 μm per layer. Exposure time varied from 6 to 30 s (135 to 675 mJ cm<sup>-2</sup>) per layer according to different composition of Z-gel solutions. The octopus demo we printed was printed at 14 s (315 mJ cm<sup>-2</sup>) per layer of 50 μm.

## **Rheology**

Rheological measurements were carried on Anton Paar Physica MCR 301 rheometer (10mm parallel plate, at 25°C), equipped with a solvent evaporation blocking kit to reduce the water loss in the tests. Strain amplitude sweeps were performed under fixed angular frequency (10 rad/s) from 0.1 to 1000 % strain and viscosity, storage (G') and loss (G'') moduli were recorded. For temperature sweeps, strain and frequency were fixed at 1 % and 1 Hz, respectively. A heating-cooling cycle were used from 4 to 70°C. To prevent the water loss, mineral oil was sprayed around the hydrogel disk after it was loaded on the instrument.

## **Characterization**

Hydrogels were dried on the lyophilizer for at least 24 hours prior to any characterizations. For NMR analysis no MBA was added. <sup>1</sup>H nuclear magnetic resonance (NMR) spectroscopy was performed on a Bruker BioSpin AVANCE 400 instrument (Bruker Co.,

Billerica, MA). NMR samples were prepared by dissolving dried uncrosslinked hydrogels in deuterium oxide at 10 mg mL<sup>-1</sup>.

Molecular weight of the non-crosslinked polymers was measured by an aqueous gel permeation chromatography (GPC) system (Waters, Milford, MA), coupled with Ultrahydrogel column and a refractive index detector. Freeze-dried samples were dissolved in phosphate buffer saline prior to the tests.

Differential scanning calorimetry (DSC) measurements and thermal gravity analysis (TGA) were performed on both dried and as prepared hydrogels using a TA Q200 DSC, and a Q500 TGA (TA Instruments, New Castle, DE), respectively.

### **Tensile Tests**

Tensile tests were performed using a Zwick/Roell Z010 testing system (Ulm, Germany) in accordance with ASTM D638. Testing samples were fabricated within a transparent Sylgard184 mold with gauge lengths of 13 mm, thicknesses of 1.5 mm, and widths of 3.8 mm. After measuring the dimensions of each testing coupon, samples were tested at a strain rate of 10 mm min<sup>-1</sup>. Stress values were calculated at each point using a constant volume approximation. Samples that failed in the gripped region were discarded to ensure that results accurately reflected uniaxial tension. The resilience of the hydrogel was measured by cyclic tensile tests up to 100 cycles, in each of which the as prepared dog-bone shaped Z-gel was elongated to  $\gamma=1$  (100% strain) at the speed of 10% per min under a controlled strain mode.

### **Photo-rheology and Photo-DSC**

Photopolymerization behavior was studied using a DHR3 Rheometer with a photocuring attachment (TA Instruments). In this experiment, a light guide directed the light source

(Omniscure Series 1500, Lumen dynamics) through a 20 mm transparent acrylic bottom plate onto the sample. The rheometer head (aluminum, 20 mm diameter, flat plate) and sample are covered with a shield to prevent unwanted exposure from ambient light. The viscosity as well as  $G'$  and  $G''$  were continuously recorded during the real-time exposure at 25 °C to determine the gelation time, which was measured when  $G'$  passes 1Pa. The frequency and strain of the measurements were fixed at 1 Hz and 10 %, respectively.

Photo-DSC was performed on a Q1000 Modulated DSC (TA Instruments), equipped with a UV Curing module with a UV light source (Omniscure Series 1500). The pre-gel solution was loaded in open aluminum pan to compare with the reference pan at 25 °C. Two waveguides aligned over the sample and reference pans directed light from the source with a measured photoirradiation density  $\sim 10 \text{ mW cm}^{-2}$ .

### **Swelling Ratio Measurement**

The swelling ratio ( $q$ ) of hydrogels was calculated by weighing the difference between the fully swollen and the as-prepared gels. Briefly, we prepared hydrogels in 10 mm diameter wells and weighed thereafter as  $W_0$ . These hydrogel disks were then soaked in 37 °C DI water for 48 hours until they reach the equilibrium state. We then weighed the fully hydrated samples as  $W_s$ . The swelling ratio was calculated as equation 1.

$$q = \frac{W_s}{W_0} \quad (1)$$

### **Design of Experiment (DOE) and Multivariate Statistical Analyses**

We applied Design of experiment (DOE) for estimating the influences of multiple SLA factors to the gelling performance, mechanical properties and swelling behavior of the resulting hydrogels.

Response surface methodology (RSM) is an effective and efficient tool in DOE for complicated multivariate analyses. In RSM, the effects of various factors and their interactions are interpreted by mathematical models, in which the coefficients are determined by nonlinear regression analysis (Eq. 2).

$$y=f (X_1, X_2, X_3,\dots X_n)+\varepsilon \quad (2)$$

$n$  represents the number of input variables;  $\varepsilon$  represents other variables such as constant coefficient or measurement error.

Firstly, we applied a simplex-centroid mixture design to determine the ratio of photoinitiator and coinitiator for the fast gelation. Using the efficient combination of riboflavin and TEOHA, we then applied Box-Behnken and inscribed central composite designs (CCD) to determine the effects of major components (monomer content and crosslinker content) and photoirradiation dosage on the output hydrogels. Levels of each component in the design were determined by preliminary experiments. Response surfaces and quadratic regression equations (Eq. 3) were then generated based on the experimental data, and thereafter used to predict the mechanical properties of the future resulting hydrogel according to specific composition. The DOE and the nonlinear regression analyses were performed by Minitab Program (Minitab Inc., Minitab release 17.2, 2015).

$$E(Y) = \beta_0 + \sum_i \beta_i X_i + \sum_i \beta_{ii} X_i^2 + \sum_i \sum_j \beta_{ij} X_i X_j$$

( $i=1, 2, 3, 4$  and  $i < j$ )

(3)

## **Antifouling Tests**

Antifouling measurements were carried out by measuring target protein absorption, as reported previously [2]. Briefly, samples of 1 mol% crosslinked zwitterionic and the AAm hydrogel with the diameter of 5 mm and thickness of 2 mm were prepared. After pre-soaking in PBS buffer overnight, hydrogel samples were immersed in 250  $\mu\text{l}$  of 1 mg  $\text{mL}^{-1}$  bovine serum albumin (BSA) solution (in PBS buffer, pH=7.4) on a 96-well plate for 6 hours at 25°C and 60% humidity. Afterwards, we performed Bradford Assay by mixing 250  $\mu\text{l}$  of Coomassie Protein Assay (Thermo Fisher Scientific) with a 5 $\mu\text{l}$  of the hydrogel-soaked BSA solution, followed by 10 min incubation at room temperature. The amounts of BSA were measured from the absorption with a spectrophotometer at the wavelength of 595 nm, and calculated according to a calibration curve. The values for each hydrogel are the mean of quintuplicate samples.

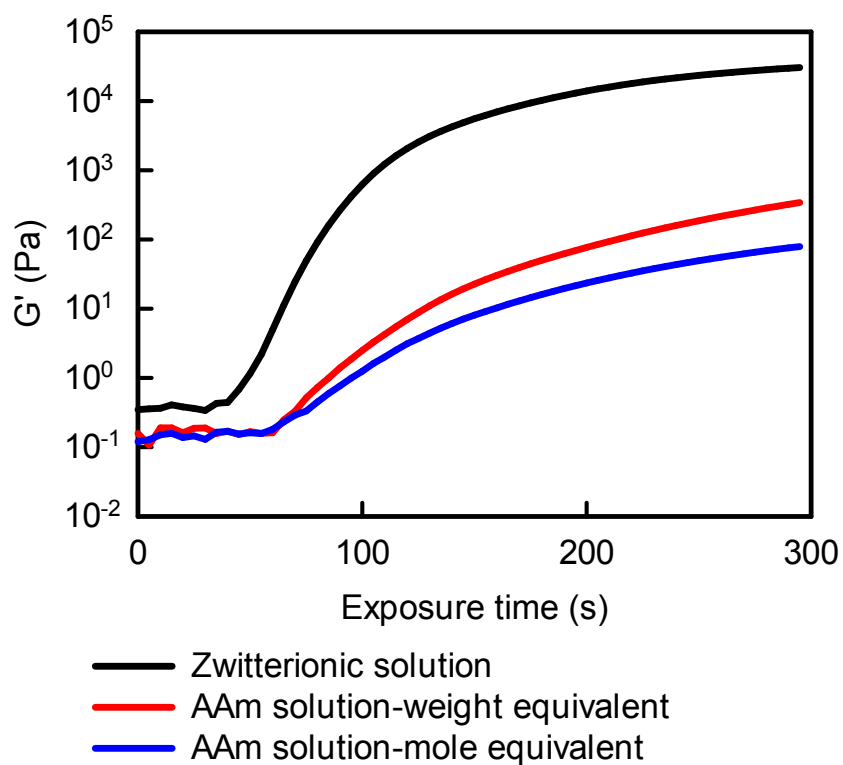
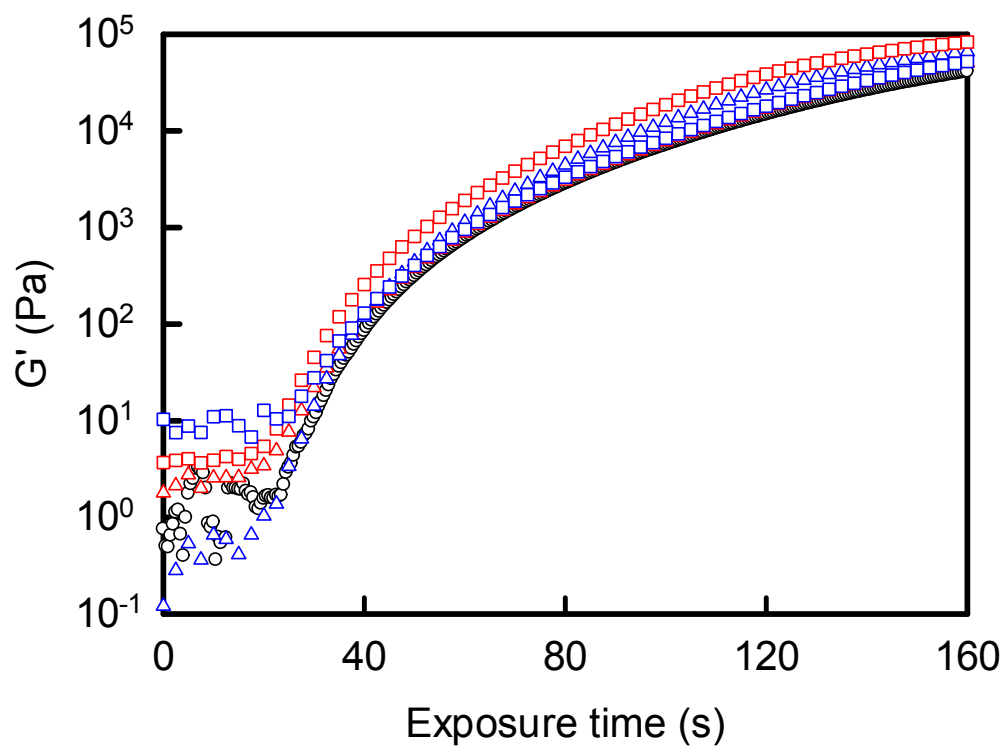


**Figure S1** Measurements of  $G'$  of the Z-gel pre-gel solution during the photopolymerization, in comparison to both the weight and molar equivalent AAm solutions, respectively. In order to minimize the impact of the chemical crosslinker,  $C_{MBA}$  was kept at the minimal level ( $\sim 0.011\text{M}$ ). The results clearly showed that the advantage of zwitterionic comonomer in gelation rate due to the presence of ionic interactions.

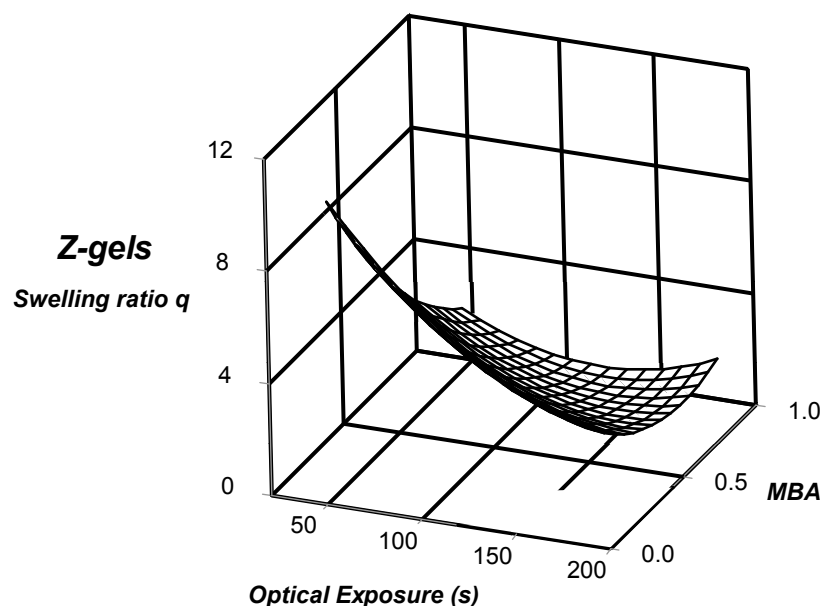


- Zwitterionic control
- △  $[\text{Ca}^{2+}]: [-\text{SO}_3^-]=1:2$
- △  $[\text{Ca}^{2+}]: [-\text{SO}_3^-]=1:4$
- $[\text{Na}^+]: [-\text{SO}_3^-]=1:1$
- $[\text{Na}^+]: [-\text{SO}_3^-]=1:2$

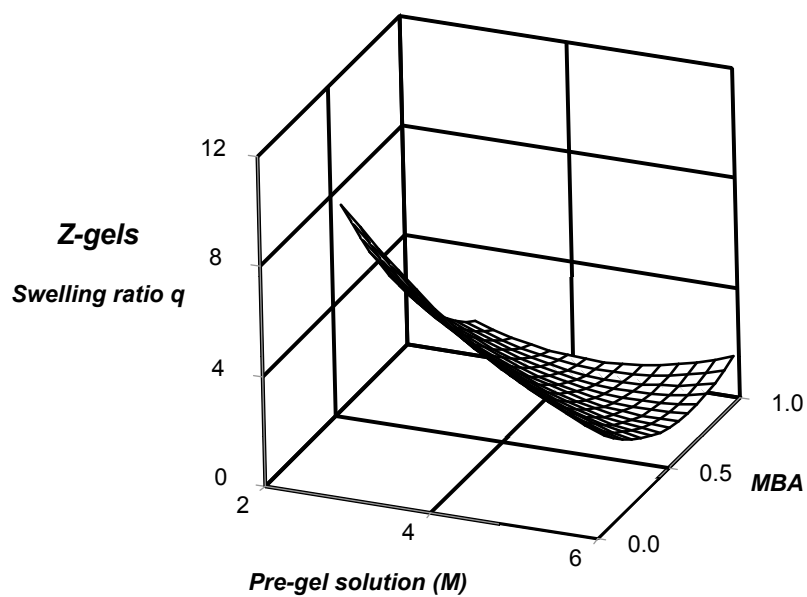
**Figure S2** Photo-rheological analyses of Z-gels with monovalent ( $\text{Na}^+$ ) or divalent ( $\text{Ca}^{2+}$ ) chloride salts at different molar ratios to the sulfonate groups in the pre-gel solutions.



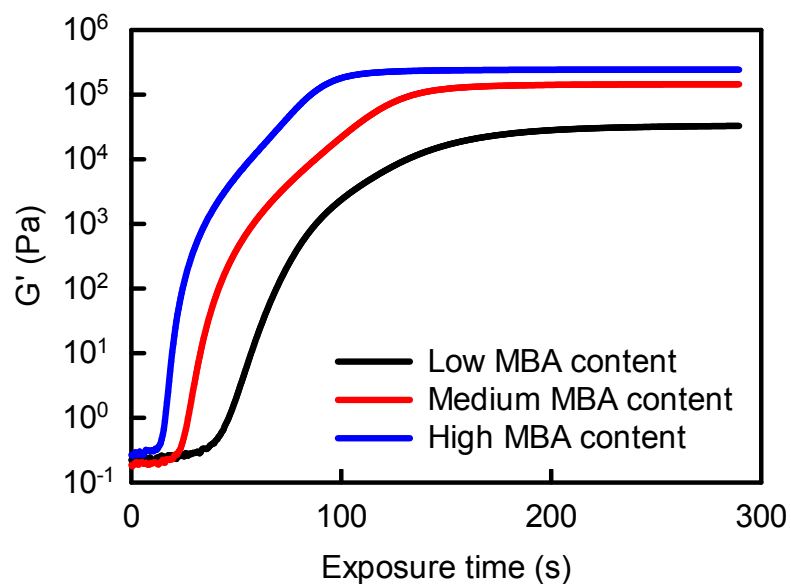
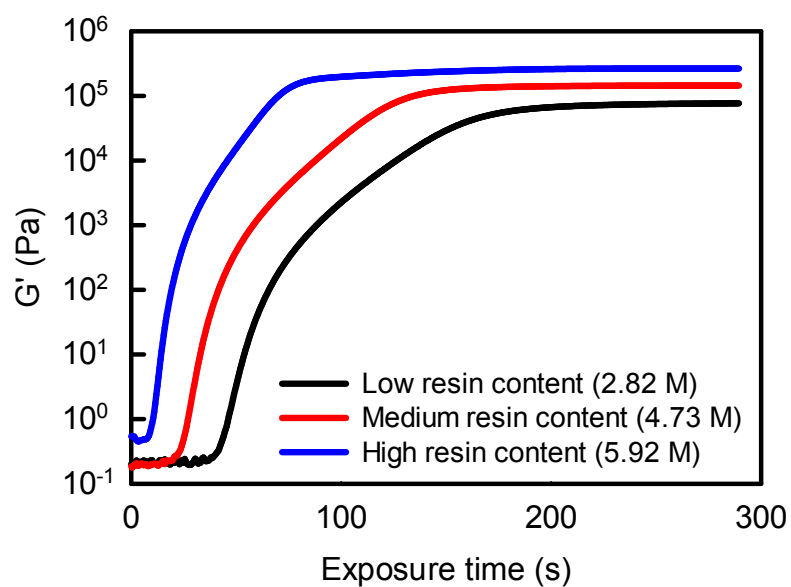
**A**



**B**



**Figure S3** The response surface plots of swelling ratio ( $q$ ) of the Z-gels, based on a three-factor Box-Behnken design: **A.** the response surface of  $q$  versus  $t_{exp}$  and  $C_{MBA}$ ; **B.** the response surface of  $q$  versus  $C_{resin}$  and  $C_{MBA}$ .

**A****B**

**Figure S4** Comparison of the gelation performance of Z-gels with different monomer content and MBA content on the photo-rheometer, with a fixed strain and fixed angular frequency: **A**. All the zwitterionic solutions had the same resin content ( $C_{resin}=4.73$  M). **B**. All the solutions contained the same  $C_{MBA}$  (1.5 mol%).

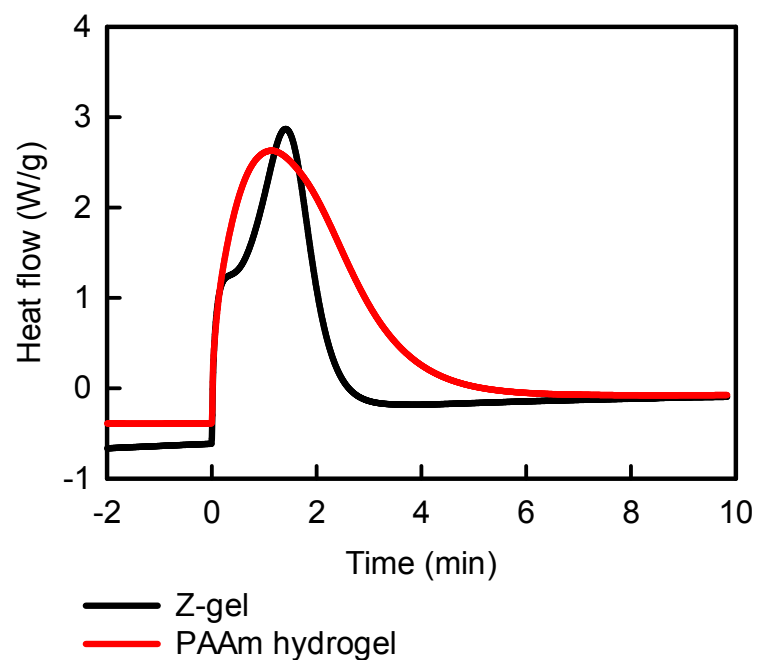


**Figure S5** Photo-DSC analysis of the polymerization of zwitterionic and AAm pre-gel solutions. All solutions contained 0.045 M MBA. The illumination started after a 2-min equilibration procedure (-2 to 0 min). The curves were calibrated by subtracting the heat flow with the background which was obtained by running the same solutions without illumination on the photo-DSC.

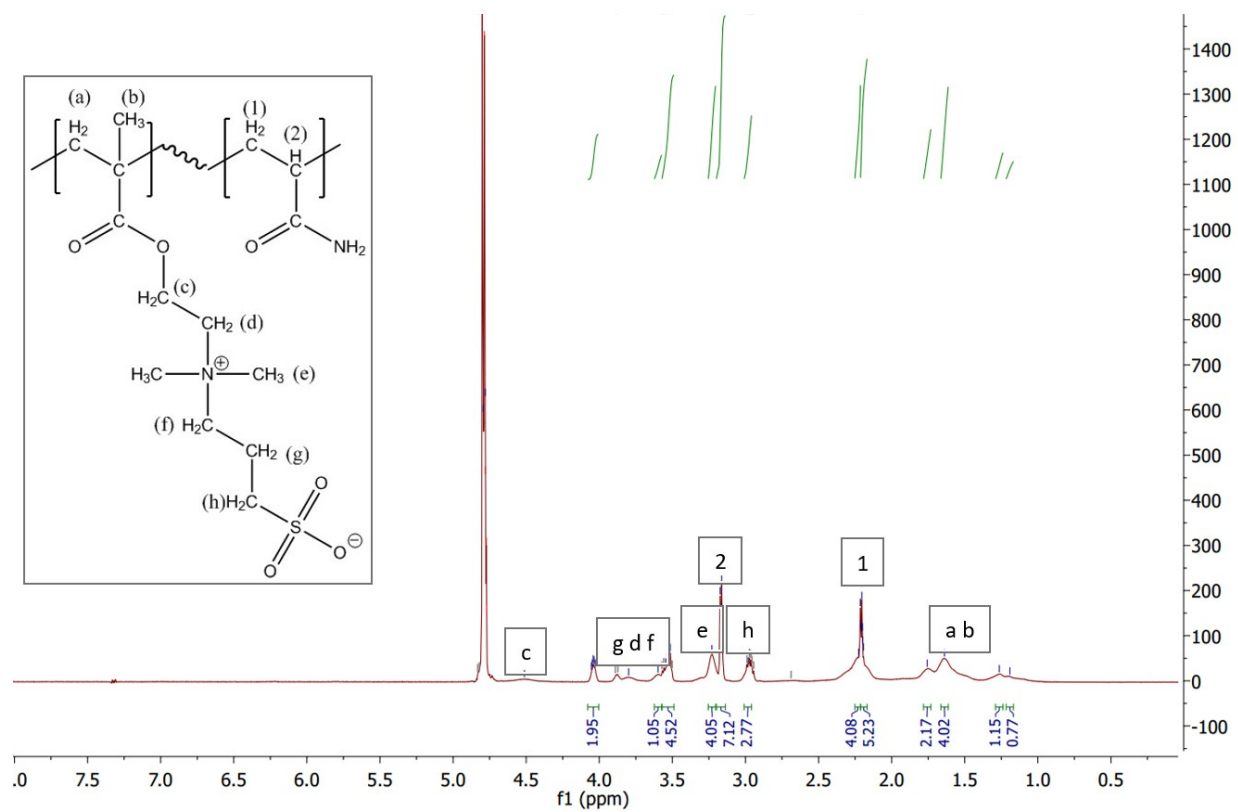
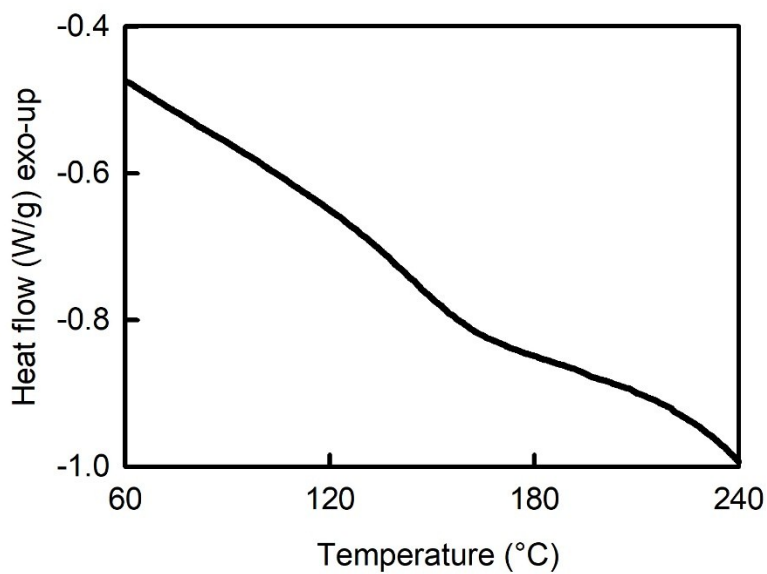


**Figure S6** NMR spectrum of the zwitterionic copolymer in the formulation. No MBA was added into the pre-gel solution. Dried polymer was dissolved in deuterium oxide.

A



B

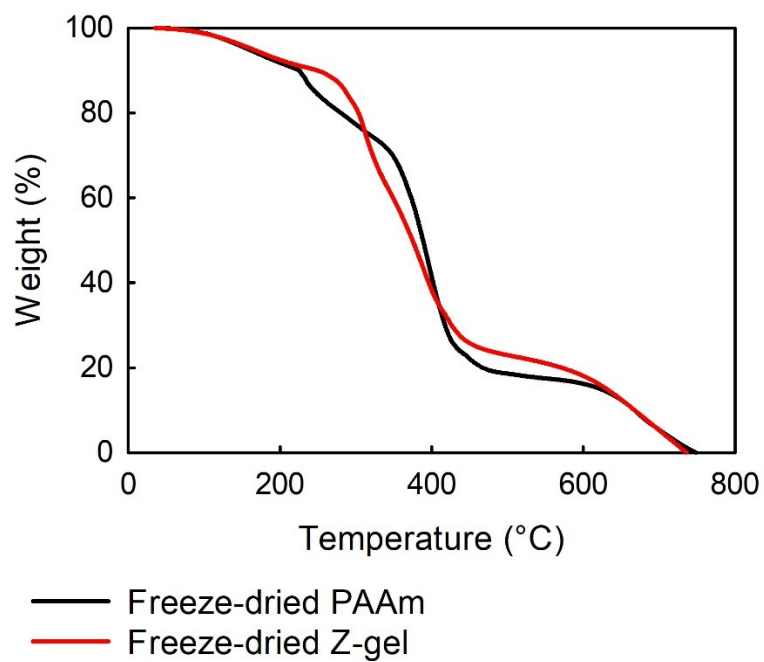


**Figure S7 Thermal analyses of the freeze-dried hydrogels by DSC and TGA. A.** DSC measurement of dried Z-gel showed glass transition at  $\sim 146.3^{\circ}\text{C}$  (onset at  $139.4^{\circ}\text{C}$  and offset at  $160.1^{\circ}\text{C}$ ). **B.** TGA of dried PAAm and Z-gel.

**Table S1.** ANOVA of Young's modulus of Z-gels by Box-Behnken design

Factor	DF	Coefficients for coded factors*	F-Value	p-Value
Model	9		51.6	0.000
Linear	3		12.8	0.009
Exposure	1	7.7E+03	21.5	0.006
MBA	1	159.1	0.2	0.695
Monomer	1	1.6E+05	16.8	0.009
Square	3		12.0	0.010
Exposure*Exposure	1	178.3	8.9	0.031
MBA*MBA	1	12.1	14.6	0.012
Monomer*Monomer	1	3.2E+04	18.0	0.008
2-Way	3		10.3	0.014
Exposure*MBA	1	30.8	5.5	0.066
Exposure*Monomer	1	3.2E+03	24.5	0.004
MBA*Monomer	1	152.2	1.0	0.353
Error	5			
Total	14			

$R^2 = 98.9\%$ , adjusted  $R^2 = 97.0\%$ ,

\* Coded factors refer to the factors coded by the Box-Behnken design, in which the upper limit of the factor is coded as 1 and the lower limit is coded as -1.

**Table S2.** ANOVA of the ultimate yield strain (represented by %) of Z-gels by Box-Behnken design

Factor	DF	Coefficients for coded factors*	F-Value	p-Value
Model	9		110.6	0.000
Linear	3		21.8	0.003
Exposure	1	2.9E+03	25.7	0.004
MBA	1	823.0	39.1	0.002
Monomer	1	8.2E+03	0.4	0.565
Square	3		8.0	0.024
Exposure*Exposure	1	8.8	18.4	0.008
MBA*MBA	1	0.3	7.1	0.045
Monomer*Monomer	1	2.3E+03	0.8	0.413
2-Way	3		32.2	0.001
Exposure*MBA	1	18.8	17.2	0.009
Exposure*Monomer	1	1.2E+03	31.9	0.002
MBA*Monomer	1	352.0	47.6	0.001
Error	5			
Total	14			

$R^2 = 99.5 \%$ , adjusted  $R^2 = 98.6 \%$ ,

\* Coded factors refer to the factors coded by the Box-Behnken design, in which the upper limit of the factor is coded as 1 and the lower limit is coded as -1.

**Table S3.** ANOVA of the gelation initiation of Z-gels by central composite design

Factor	DF	Coefficients for coded factors*	<i>F</i> -Value	<i>p</i> -Value
Model	5		135.5	0.000
Linear	2		26.8	0.001
Monomer	1	305.0	0.1	0.779
MBA	1	72.9	53.6	0.000
Square	2		26.4	0.001
Monomer*Monomer	1	137.0	0.4	0.566
MBA*MBA	1	0.6	41.8	0.000
2-Way	1		67.7	0.000
MBA*Monomer	1	31.7	67.7	0.000
Error	7			
Total	12			

$R^2 = 99.0 \%$ , adjusted  $R^2 = 98.2 \%$ ,

\* Coded factors refer to the factors coded by the CCD.



**Table S4.** ANOVA of the gelation initiation of PAAm hydrogels by central composite design

Factor	DF	Coefficients for coded factors*	F-Value	p-Value
Model	5		139.8	0.000
Linear	2		11.3	0.006
Monomer	1	1.5E+04	17.5	0.004
MBA	1	-67.4	4.8	0.065
Square	2		99.2	0.000
Monomer*Monomer	1	3.07E+03	18.2	0.004
MBA*MBA	1	3.2	116.3	0.000
2-Way	1		0.6	0.474
MBA*Monomer	1	-9.1	0.6	0.474
Error	7			
Total	12			

$R^2 = 99.0 \%$ , adjusted  $R^2 = 98.3 \%$ ,

\* Coded factors refer to the factors coded by the CCD.

## References

- [1] Peele BN, Wallin TJ, Zhao H, Shepherd RF. 3D printing antagonistic systems of artificial muscle using projection stereolithography. *Bioinspiration & biomimetics*. 2015;10:055003.
- [2] Chen K, Zhou S, Wu L. Self-Healing underwater superoleophobic and antibiofouling coatings based on the assembly of hierarchical microgel spheres. *ACS nano*. 2015;10:1386-94.